Available online at www.sciencedirect.com
SCIENCE DIRECT
Tectonophysics 411 (2005) 157–167
TECTONOPHYSICS
www.elsevier.com/locate/tecto

The misorientation index: Development of a new method for calculating the strength of lattice-preferred orientation

Philip Skemer *, Ikuo Katayama, Zhenting Jiang, Shun-ichiro Karato

Department of Geology and Geophysics, Yale University, PO Box 208109, New Haven, CT 06520-8109, USA

Received 13 June 2004; accepted 19 August 2005
Available online 2 November 2005

Abstract

Using orientation data from experimentally deformed olivine, we explore some practical problems with the J-index, a commonly applied measure of fabric strength. We show that the J-index is highly dependent on several factors, including the number of discrete data in the orientation distribution function (ODF), and arbitrary numerical parameters specified for its calculation. Because of this non-uniqueness, we conclude that the J-index is difficult to interpret and should only be applied with caution. As an alternative to the J-index, we propose a new measure of fabric strength that is based on the distribution of uncorrelated misorientation angles. This "M-index" is shown to be insensitive to the parameters specified for its calculation. For typical deformed olivine samples, we show that ~150 discrete data are adequate to quantify fabric strength using the M-index technique. The M-index correlates well with seismic anisotropy, particularly for materials of the same fabric type. Therefore, we conclude that the M-index technique is well-suited for the quantification of fabric strength and the comparison of like materials.

Keywords: Olivine; Anisotropy; J-index; M-index; Texture index; Misorientation angle; Lattice-preferred orientation; Fabric strength

1. Introduction

Studies of the lattice-preferred orientation (LPO) of experimentally and naturally deformed materials provide crucial insight into geodynamic processes. LPO is critical to our interpretation of seismic data, which in turn illuminates the nature of dynamics and kinematics in Earth (e.g., Nicolas and Christensen, 1987; Karato, 1987). However, the study of LPO has been hindered by imperfect methods for describing the strength of fabrics. Typically, LPO is represented by pole figures, which show the orientations of individual grains with respect to an external reference frame (e.g. Wenk, 1985). Although variations in fabric strength can be observed qualitatively from a pole figure, there is no robust method for the quantitative determination of fabric strength. For practical purposes, it is desirable to have an index that 1) provides a quantitative indication of fabric strength, 2) is free of numerical artifacts, 3) is comparable across different studies, and 4) is easy to apply and interpret.

The J-index, defined by Bunge (1982), is a commonly applied measure of fabric strength in the geological and materials science literature (e.g. Mainprice and Silver, 1993; Ben Ismail and Mainprice, 1998). Mathematically, it is defined as the second moment of an orientation distribution function (ODF), where an ODF is the distribution of discrete crystal orientation data in Euler angle space. Although its formulation is straightforward, the J-index is known to be difficult to interpret because it is highly sensitive to the number of grains measured and

* Corresponding author. Tel.: +1 203 605 3409.
E-mail address: philip.skemer@yale.edu (P. Skemer).

0040-1951/$ - see front matter © 2005 Elsevier B.V. All rights reserved.
doi:10.1016/j.tecto.2005.08.023

arbitrary smoothing factors applied in its calculation (Matthies and Wagner, 1996; Wenk, 2002). In fact, Wenk (2002) argued that an impractically large number of discrete orientation data would be needed to obtain a meaningful measure of fabric strength using the J-index technique. In this paper, we investigate the J-index problem in greater detail. Using orientation data from experimentally deformed olivine, we systematically examine the dependence of the J-index on several factors, including the number of discrete data in the ODF and numerical parameters specified for its calculation. We find that the J-index is indeed sensitive to these factors, and conclude that the J-index is an ambiguous indicator of fabric strength.

As an alternative to the J-index we propose a new measure of fabric strength that is based on the distribution of misorientation angles. A misorientation angle is the angle of rotation around a common axis required to bring two crystal lattices into the same orientation. By convention, the smallest possible angle is chosen to represent the misorientation of two lattices (Wheeler et al., 2001). When two grains have a similar orientation, their misorientation angle is small; if their orientations are identical, their misorientation angle is zero. When two grains have highly dissimilar orientations, their misorientation angle is large, with a maximum value that depends on crystal symmetry (e.g. Grimmer, 1979). In the case where fabric is strong, many grains have similar orientations. Thus, the distribution of misorientation angles is dominated by small angles. With increasing deformation and LPO development, the distribution of misorientation angles is known to shift towards low angles, as grains become increasingly aligned (e.g. Wheeler et al., 2001). This shift in the distribution of misorientation angles provides a physical basis for the misorientation-index (M-index), which we introduce here. Using orientation data from experimentally deformed olivine, we find that the M-index is a robust measure of fabric strength and is insensitive to the numerical parameters used in its calculation. For experimentally deformed olivine samples of typical fabric strength, we show that meaningful results can be obtained for a small number of discrete orientation measurements (~150 grains).

2. Methods

2.1. Orientation measurements

To evaluate the numerical behavior of the J-index and the M-index we use orientation data from four olivine samples of different fabric strengths. Olivine was chosen because of its abundance in the upper mantle and the significance of its contribution to upper mantle seismic anisotropy. An isostatically annealed olivine polycrystal of near random fabric represents a lower limit of fabric strength. Data from three olivine samples experimentally deformed to various shear strains represent a range of increasing fabric strengths. These samples were deformed in simple shear under conditions where the [100](001) slip system dominates strain accommodation. For details of these deformation experiments see Katayama et al. (2004). The LPO of each sample was measured using the electron backscatter diffraction (EBSD) technique on an FEI XL-30 ESEM-FEG. The angular resolution of data acquired using the EBSD technique is one degree or better (Prior et al., 1999). Kikuchi patterns were indexed automatically using Channel 5+ software by HKL Technology. An accelerating voltage of 20 kV and a current of 2.4 nA were used at a working distance of 20 mm.

2.2. Calculation of fabric strength and seismic anisotropy

2.2.1. J-index calculation

Orientation distribution functions (ODFs) and associated J-indices were calculated from EBSD data. The J-index is defined by Bunge (1982) as:

$$J \equiv \int [f(g)]^2 \mathrm{d}g \qquad (1)$$

where $f(\phi_1,\psi,\phi_2)$ is the ODF, ϕ_1,ψ,ϕ_2 are the Euler angle representations of the orientation data, and dg is a volume element in Euler angle space. By definition, the J-index ranges from unity (corresponding to a completely random fabric) to infinity (a single crystal fabric). J-indices were calculated using the commonly applied method in which the ODF is expanded into a series of spherical harmonics. Practical application of this technique requires that the expansion is truncated at a finite number of terms. Additionally, a Gaussian smoothing function can be applied, which replaces discrete points with a Gaussian probability distribution centered on the data. The Gaussian half-width (GHW) is defined as the angular distance over which the probability decreases by a factor of $1/e$. With all ODF calculations it is necessary to specify a bin size in Euler angle space. Calculation times increase rapidly with decreasing bin size, so there are some practical limitations in this regard. We chose a bin-size (5.625°) that was fine enough to allow accurate reproduction of

the ODF, while still being sufficiently coarse to permit reasonable calculation times.

The numerical parameters specified for the calculation may influence the ultimate value of the J-index; in this study, we seek to understand the importance of these effects. The dependence of the J-index on the GHW and the truncation of the spherical harmonic expansion is determined by evaluating a single sample with a constant number of grains for combinations of these two parameters. We investigated GHWs from 0° to 90°, and a spherical harmonic expansion truncated at degree 2 to 34. We investigated all possible combinations of these parameters to obtain a complete picture of parameter space. However, it should be emphasized that not all combinations of parameters give significant results. If data are artificially filtered or smoothed, increasing the number of terms in the spherical harmonic expansion beyond a certain threshold does not provide any additional description of the ODF. This threshold is reached when the magnitude of smoothing exceeds the scale of the features described by the highest order harmonic, which corresponds roughly to GHW $\geq \pi/l$ where l is the degree of the highest order harmonic.

The influence of the number of discrete data on the J-index calculation was determined by holding the other numerical parameters constant and calculating J-indices for incremental subsets of orientation data. For each sample, the data were initially randomized to avoid any artifact of the sampling procedure. From this randomized data set, incremental subsets were generated by selecting grains 1 through 25; 1 through 50; 1 through 75; etc.

2.2.2. M-index calculation

There are two classes of misorientation angles. Correlated misorientation angles are the set of all misorientation angles calculated from grain pairs in direct contact. Uncorrelated misorientation angles are calculated from the complete set of all possible grain pairs, including those that are not in direct contact (e.g. Wheeler et al., 2001). Thus, the set of uncorrelated misorientation angles contain information about the relationships between each grain and every other grain in a sample. Misorientation angles have been applied to qualitatively describe fabric strength and infer deformation mechanisms in naturally deformed rocks and experimentally deformed metals and ceramics (e.g. Liu and Chakrabarti, 1996; Fliervoet et al., 1999; Jiang et al., 2000; Lapworth et al., 2002). They have also been modeled numerically and studied experimentally to predict the distribution of uncorrelated misorientation angles for a random fabric (MacKenzie and Thomson, 1957; Grimmer, 1979; Samajdar and Doherty, 1994; Morawiec, 1995). Some workers have compared their observed data to these theoretical distributions using statistical chi-squared tests to draw conclusions about the randomness of fabric (e.g. Fliervoet et al., 1999). However, to our knowledge, there has been no attempt to use the distribution of misorientation angles as a quantitative indicator of fabric strength for a full range of deformed samples. Most prior work, due to computational constraints, chose random subsets of a larger data set of uncorrelated misorientation angles, limiting their analyses to several hundred misorientation angles (e.g. Jiang et al., 2000; Lapworth et al., 2002). We were not restricted in this regard and used up to 600,000 uncorrelated misorientation angles in our analyses.

We define the misorientation index (M-index) as the difference between the observed distribution of uncorrelated misorientation angles and the distribution of uncorrelated misorientation angles for a random fabric:

$$M \equiv \frac{1}{2} \int |R^T(\theta) - R^0(\theta)| \mathrm{d}\theta . \quad (2)$$

The practical calculation is made for individual bins: $M \equiv \sum_{i=1}^{n} | R_i^T - R_i^0 | \cdot \frac{\theta_{\max}}{2n}$, where R_i^T is the theoretical distribution of misorientation angles for a random fabric, R_i^0 is the observed distribution of misorientation angles (normalized by the number of data), $\theta_{\max}$ is the maximum theoretical misorientation angle, and n the number of bins. The factor of 1/2 is for convenience, so that the magnitude of the index increases with fabric strength from 0 (random fabric) to 1 (single crystal fabric). Individual misorientation angles were calculated from EBSD data. The complete set of all uncorrelated misorientation angles was compiled and a distribution was calculated for a given bin size (generally 1° bins were used). This observed distribution was then subtracted from the appropriate theoretical distribution for a random fabric, to give a value for the M-index. The theoretical distribution for a random fabric depends on crystal symmetry and bin width. We use the distribution for orthorhombic crystals from Grimmer (1979).

To test for possible numerical artifacts in this calculation, incremental subsets of data were analyzed to determine the number of grains necessary for this type of analysis. A range of bin sizes was also investigated to ensure that the choice of bin-size did not significantly influence the results.

2.2.3. Seismic anisotropy calculation

Seismic anisotropy was calculated from Euler angles (Mainprice, 1990) and elastic constants for San Carlos

olivine at room pressure and temperature (Abramson et al., 1997). The incremental subsets of Euler angle data were analyzed to investigate the dependence of seismic anisotropy calculations on the number of discrete data.

3. Results

3.1. J-index

If the J-index can be calculated in a way that is free of numerical artifacts, there must be a region in parameter space where the J-index has a unique value that is independent of the parameters specified in its calculation. Fig. 1 shows how the J-index depends on the GHW and the degree of the highest order spherical harmonic. The gray region represents combinations of parameters where the smoothing exceeds the resolution of the highest order spherical harmonics; these points can be neglected in subsequent discussion. From Fig. 1, it is clear that the J-index varies continuously throughout parameter space. In general, J-indices increase with decreasing GHW, and increase with increasing spherical harmonic order. At small GHWs, the J-index continuously increases with increasing spherical harmonic order as data become increasingly well described. At constant spherical harmonic order and increasing GHW, the J-index decreases asymptotically towards unity as the details of the ODF become obscured.

In addition to the dependence of the J-index on the numerical parameters used in its calculation, the magnitude of the J-index depends on the number of discrete data in the ODF. Fig. 2 shows the behavior of the J-index when plotted against $1/N$, where N is the number of grains in the analysis. Matthies and Wagner (1996) and Wenk (2002), have argued that the J-index always decreases linearly with $1/N$, implying that no finite number of grains will give a real value for the J-index. We find, however, that these plots can be roughly classified into two categories, depending on the strength of the fabric and the numerical parameters used in the calculation. For weak fabrics, the J-index decreases with an increasing number of data, proportionately to $1/N$. This is most apparent for the nominally undeformed, hot-pressed olivine sample (Fig. 2a1–a3). However, for strong fabrics, the J-index appears to converge to a certain value for a finite number of data. This behavior is illustrated in Fig. 2c1–c3, for the highly deformed sample GA-25. Note, however, that even in

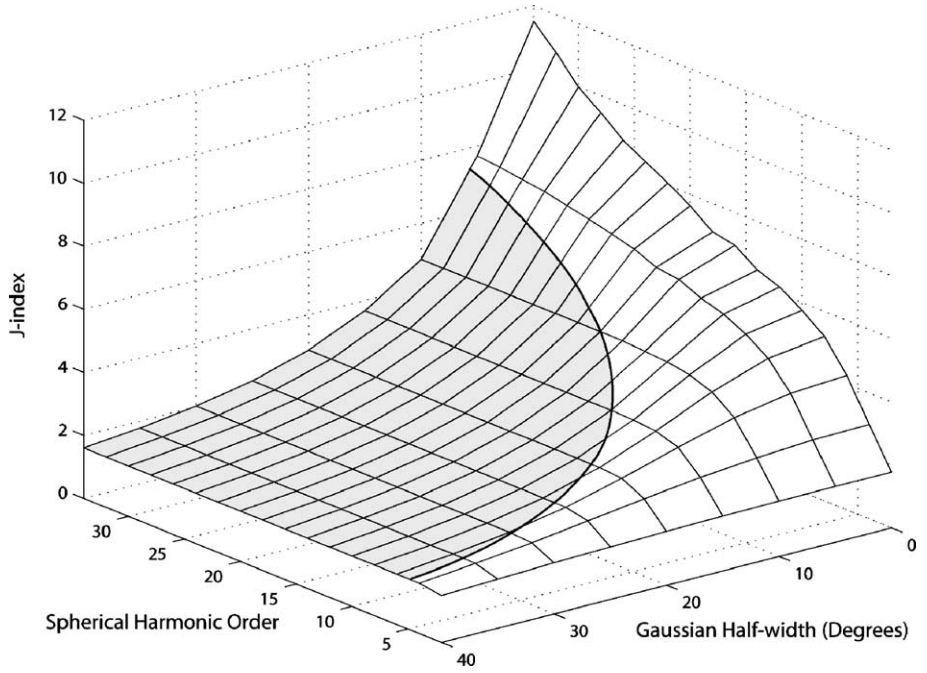

Fig. 1. The relationship between the J-index, Gaussian half-width (GHW), and the degree of the highest order spherical harmonic. All calculations were done for a single sample (GA-25) and a constant number of grains ($N=378$). The gray region represents points where the degree of smoothing exceeds the resolution of the highest order harmonics. Both the GHW and the number of spherical harmonic terms influence the magnitude of the J-index. There is no region in this parameter space where the J-index is independent of both the GHW and the number of terms in the spherical harmonic expansion.

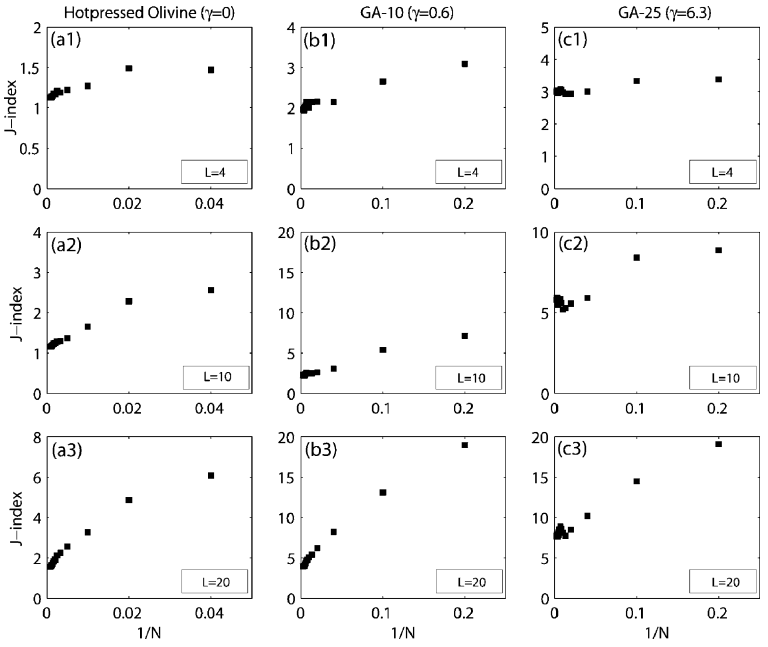

Fig. 2. The relationship between the J-index and the number of grains analyzed. The convergent behavior is illustrated by a plot of the J-index against $1/N$, where N is the number of data in the analysis. L is the degree of the highest order spherical harmonic. No Gaussian smoothing was applied to these data. These plots may exhibit different behaviors: Either these data converge to some value or they decrease linearly with respect to $1/N$. A range of fabric strengths is shown here. The hot-pressed olivine sample (a1–a3) always appears to show non-convergent behavior, while the highly deformed sample GA-25 always appears to show convergent behavior (c1–c3). Intermediately deformed sample GA-10 illustrates the transition from convergent (at $L=4$, b1) to non-convergent (at $L=20$, b3) behavior.

these cases, the asymptotic values depend on the degree of the highest order spherical harmonic. Transitional behavior is evident in the modestly deformed sample GA-10. When the spherical harmonic expansion is truncated at degree four (Fig. 2b1), the J-index appears to converge to a certain value. However, when the spherical harmonic expansion is truncated at degree twenty (Fig. 2b3), the J-index continues to decrease proportionally to $1/N$.

3.2. M-index

Fig. 3 shows distributions of misorientation angles for several samples of different fabric strengths, with pole figures of the samples for comparison. The solid lines on the distribution plots are the theoretical curves for a random fabric. With increasing fabric strength (from Fig. 3a to d), the distribution of misorientation angles shows an increased deviation from the random fabric curve and the pole figures show an increased clustering of orientation data. For the hot-pressed olivine sample, the distribution of uncorrelated misorientation angles is almost identical to the theoretical random distribution. For the deformed samples, the distribution shifts towards lower angles. With increasing strain and fabric strength, this shift is increasingly large. In the most highly deformed sample (Fig. 3d) the distribution is dominated by low angle misorientations; consequently, the M-index is quite high ($M=0.44$).

The magnitude of the M-index is dependent on the number of grains measured (Fig. 4). With an increasing number of grains, the magnitude of the M-index decreases from its single crystal value (unity) and converges towards some finite value. For the deformed olivine samples, the M-index converges at approximately 150 grains (~12000 uncorrelated misorientation angles). Beyond 150 grains, variation in the magnitude of the M-index is less than 2% of the theoretical maximum. For the undeformed sample (hot-pressed olivine), the M-index converges more slowly. For ~600 grains, $M=0.01$, which reflects the fact that the fabric is not completely random. This can also be seen in the pole figure (Fig. 3a).

To confirm that bin-size does not influence the magnitude of the M-index, we calculated the M-index of two samples at ten different bin sizes (Fig. 5). The variation is small and becomes insignificant for bin sizes smaller than 5°. Below 5°, variation is less than 0.2% of the theoretical maximum.

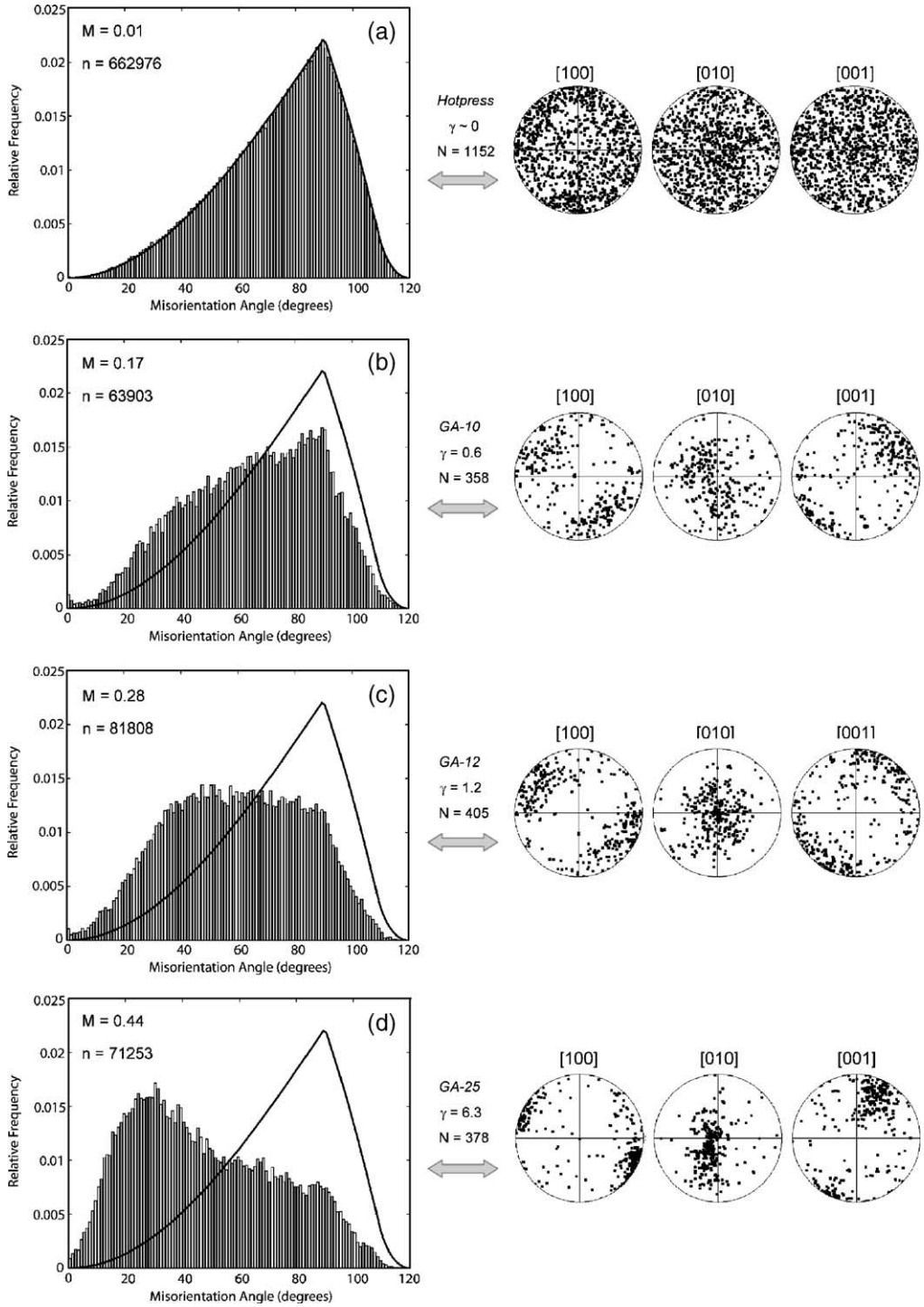

Fig. 3. The distribution of misorientation angles for each sample. Data are plotted as a normalized histogram, with the theoretical curve for a random distribution shown as a solid line. Pole figures of orientation data for each sample provide an intuitive basis for comparison. With increasing strain (γ) the distribution shifts towards lower angles and the magnitude of the M-index (M) increases. N is the number of grains; n is the number of uncorrelated misorientation angles. Fabric strength and consequently M-indices increase from (a), the hot-pressed olivine, through (d), the highly deformed GA-25.

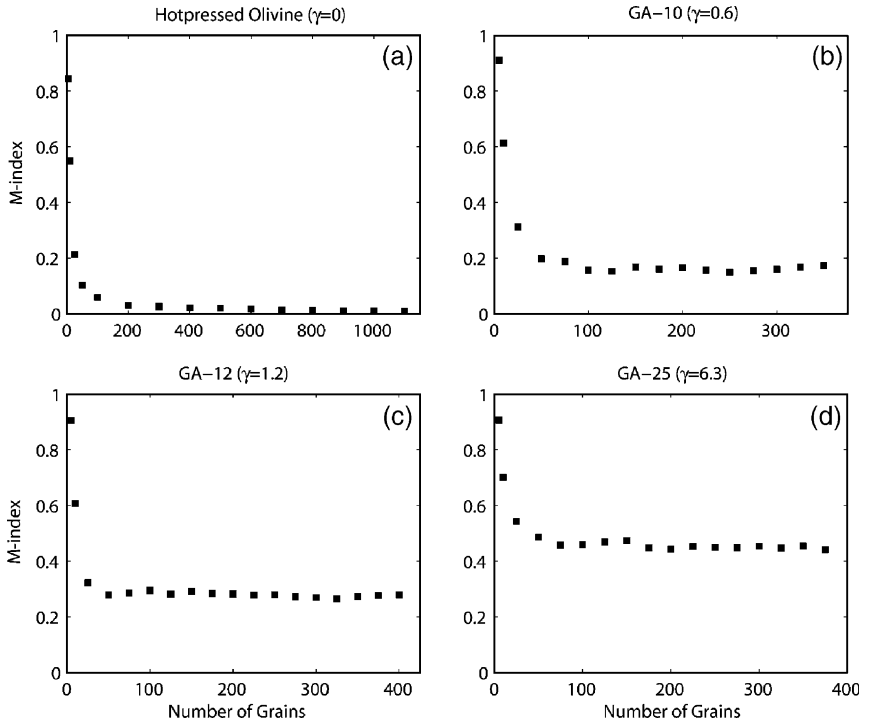

Fig. 4. The relationship between the M-index and the number of data. γ is the approximate shear strain. (a) The M-index for the hot-pressed olivine decreases from its single crystal value and converges to a finite value at approximately 600 grains. For the deformed samples (b), (c), and (d), the M-index converges to a single value at approximately 150 grains.

3.3. Seismic anisotropy

The results of seismic anisotropy calculations are shown in Fig. 6. The magnitude of seismic anisotropy is dependent on the number of grains measured, but converges at a sufficient number of grains. The number of grains necessary to observe convergence is small and depends on the strength of the fabric. In the deformed olivine samples we study here, this convergence occurs at ~150 grains. Beyond 150 grains, changes in the magnitude of anisotropy are small, typically less than 2% of the maximum anisotropy for a single crystal. For the nominally undeformed sample (hot-pressed olivine), convergence is observed for a larger number of grains (~600). These observations are generally consistent with observations of the convergence of the M-index.

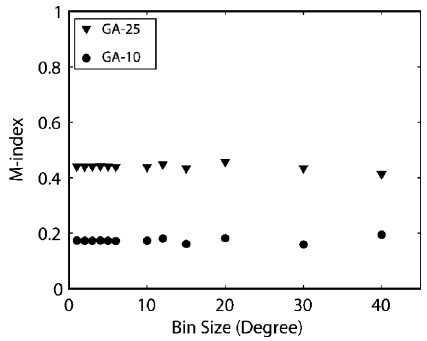

Fig. 5. The dependence of the M-index on bin-size. Samples GA-10 (●) and GA-25 (▼) exhibit similar behavior, showing little variation with bin-size. At bin-sizes less than 5°, variation in the M-index is less than 0.2% of the theoretical maximum.

4. Summary and discussion

Although the theoretical basis for the J-index is straightforward, the practical nature of its calculation is problematic. We have investigated three aspects of the J-index calculation – the number of terms in the spherical harmonic expansion, the degree of artificial smoothing (GHW), and the number of discrete orientation data – and found that each has some effect on the J-index.

In Fig. 1, when GHW=0, the J-index continually increases with increasing spherical harmonic order. Indeed, in the absence of any artificial smoothing, the J-index should continue to increase with an increasing number of spherical harmonic terms until each discrete point in the ODF is perfectly described (Bunge, 1982). The resolution of features in an ODF is determined by the number of terms in the spherical harmonic expan-

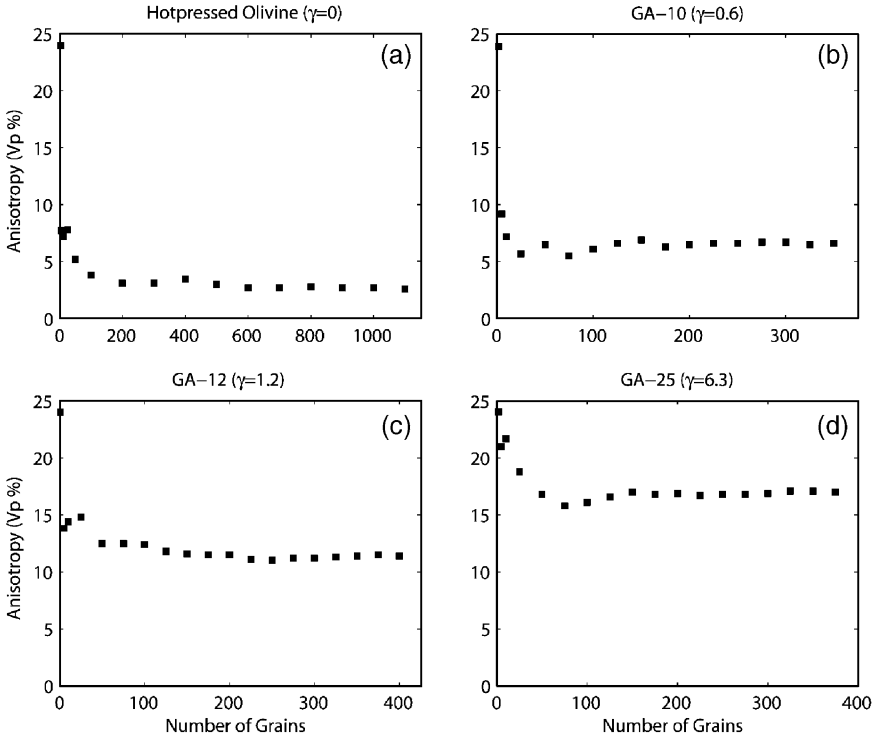

Fig. 6. The relationship between seismic anisotropy and the number of data. The seismic anisotropy plotted is percent P-wave azimuthal anisotropy. For the hot-pressed olivine (a), seismic anisotropy converges to a single value at approximately 600 grains. For the deformed olivine samples (b), (c), and (d), anisotropy converges to a single value at approximately 150 grains.

sion. Broad features can be described by low-order spherical harmonics while finer features require higher-order terms. As Bunge (1982) noted, the number of spherical harmonic terms in an ODF calculation must be chosen so that only the features of interest are described. Yet, the importance of different features in an ODF depends on the specific focus of a study. Thus, the truncation of the spherical harmonic expansion is highly arbitrary. Without a formal method for comparing J-indices calculated with different spherical harmonic truncations, it is extremely difficult to interpret reported J-index values in the geologic literature.

The ambiguity of the J-index is compounded when the effects of filtering or smoothing are considered. In this study, we documented the effects of Gaussian smoothing on our data, however similar effects will arise from the practical necessity of specifying a bin-size for the ODF. When smoothing or coarse-scale binning is applied, fine-scale details of the ODF are obscured. The advantage of smoothing or binning is that a finite number of spherical harmonic terms can adequately describe the ODF. However, any smoothing applied is arbitrary, and will have a potentially large effect on the magnitude of the J-index (Fig. 1).

Under certain conditions, we observe a proportional relationship between the J-index and $1/N$, where N is the number of discrete orientation data (Matthies and Wagner, 1996; Wenk, 2002). This behavior is most evident in weak fabrics, or fabrics that are highly smoothed. For strong fabrics, or modest fabrics described by low order spherical harmonics, the J-index appears to converge to a certain value at a finite number of grains. The $1/N$ phenomenon may be explained as follows: ODFs are subject to the normalization condition where $\int f(g)\mathrm{d}g = 1$. When a fabric is weak, f is nearly constant in Euler angle space, hence $\int f(g)\mathrm{d}g \approx f \int \mathrm{d}g = fN = 1$. Therefore, $f(g) \approx \frac{1}{N}$ and $\int f^2 \mathrm{d}g \approx f^2 \int \mathrm{d}g = \frac{1}{N}$. Thus, from the definition of the J-index (Eq. (1)), it is clear that under certain circumstances the J-index will vary proportionally to $1/N$.

In Fig. 7a,b, the J-index is plotted against P-wave azimuthal and shear-wave splitting anisotropy, respectively. Data from four samples are shown, with J-indices calculated for several combinations of numerical parameters. For each combination of parameters, there is a reasonably good correlation between the J-index and seismic anisotropy. However, the slope of each curve is different, indicating that the relationship

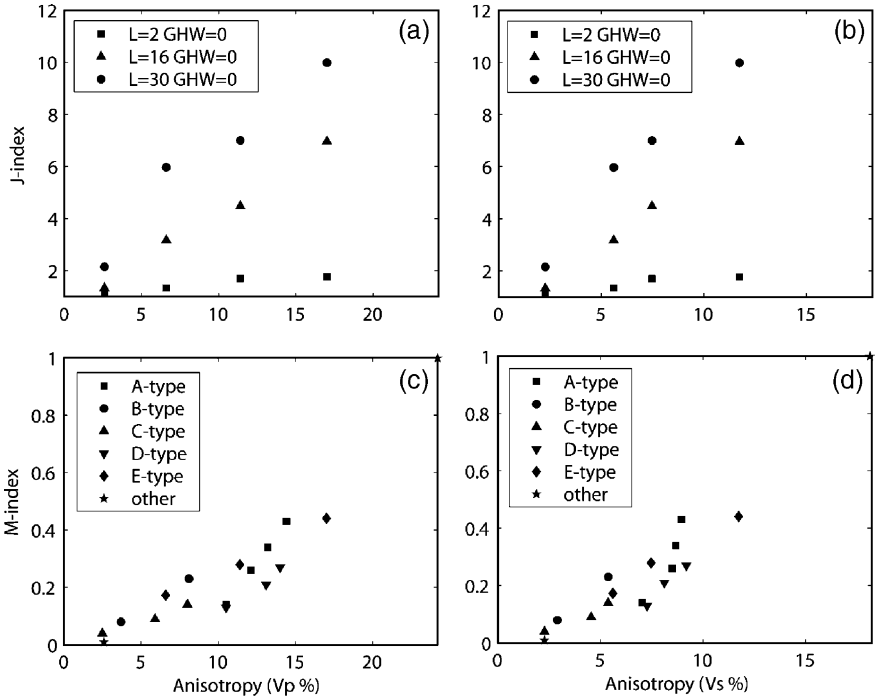

Fig. 7. The relationship between the J-index, the M-index, and seismic anisotropy. V_p anisotropy is percent azimuthal anisotropy. V_s anisotropy is percent shear-wave splitting anisotropy. (a, b) The relationship between the J-index and seismic anisotropy is shown to depend strongly on the parameters specified during the calculation. L is the degree of the highest order spherical harmonic. For simplicity, no smoothing is applied to these data (i.e. GHW=0). (c, d) While there is a general relationship between the M-index and seismic anisotropy, the exact relationship depends on the type of deformation. Data are shown for five olivine fabric types; other data include the nominally undeformed olivine hot-press and an olivine single crystal. Error in the M-index and seismic anisotropy calculations is largely a consequence of the number of data in the analysis, but is expected to be less than 2% of their respective theoretical maxima.

between the J-index and seismic anisotropy depends strongly on the specific choice of parameters applied in the calculation.

In Fig. 7c,d, the M-index is plotted against seismic anisotropy. The data in these figures are from a variety of experimental and naturally deformed olivine samples. Several fabric types are represented; they are noted using the nomenclature of Jung and Karato (2001) and Katayama et al. (2004). Unlike the J-index, the M-index is essentially independent of the parameters used in its calculation, so none are specified here. Broadly speaking, there is a positive correlation between the M-index and seismic anisotropy. There is a small degree of scatter in the data, which reflects the fact that samples with different dominant slip systems exhibit slightly different relationships between the M-index and seismic anisotropy. For samples of the same fabric type (in Fig 7c,d, those denoted by the same symbols), the correlation between the M-index and seismic anisotropy is quite good. However, this means that the M-index should only be used to draw comparisons between similar samples that deformed under similar conditions.

The numerical artifacts associated with the J-index calculation reflect the fact that three-dimensional Euler angle space is generally populated by a relatively small number of discrete data. The M-index is preferable in this regard because the data set of uncorrelated misorientation angles is large and the distribution of data is one-dimensional. Practically, we are constrained to work with a finite number of data. For example, a typical data set might contain 300 orientation measurements. In the ODF representation, these 300 data are distributed amongst several thousand bins. However, the same data set of 300 orientation measurements contains $\sim 4.5 \times 10^4$ uncorrelated misorientation angles, distributed amongst approximately 100 bins. With a large density of data, no smoothing is required to observe a continuous distribution of data, and with a simple one-dimensional function, no mathematical construct, such as spherical harmonics, is required to approximate the data. The M-index contains only two possible sources of artifact in its calculation – the number of grains and the bin width – and we have shown here that for reasonable choices of each, there is no systematic effect on the magnitude of the M-index.

5. Conclusions

The problems with the J-index can be summarized as follows: the arbitrary choice of the spherical harmonic truncation and any artificial smoothing (e.g. GHW) applied during the calculation of an ODF will have complicated effects on the magnitude of the associated J-index. Therefore, the J-index is not uniquely defined. Furthermore, for weak or highly smoothed fabrics, the J-index does not converge to a single value, remaining dependent on the number of data in the analysis. For strong fabrics, the J-index will converge to a single value, but with a value that depends on the particular parameters chosen.

The M-index is not without limitations. In particular, it should only be used to compare similar materials deformed in the same deformation geometry and with the same active slip systems. This study has also only documented the behavior of the M-index for olivine. Further research is necessary to confirm the M-index's validity or practicality for other materials. Finally, it should be noted that a scalar index can never completely characterize the intensity of fabric, because the intensity of fabric is not a scalar quantity. Both the M-index and J-index are scalars, and as such only contain partial information about a fabric.

The advent and recent popularization of electron–backscatter diffraction (EBSD) has allowed researchers to conduct more extensive microstructural and crystallographic studies on single grain scales. The ambiguity of the J-index renders more acute the need for a robust measure of fabric strength. Here we show that the M-index, based on the distribution of uncorrelated misorientation angles, describes fabric strength in a systematic manner, without being hindered by complications arising from its numerical calculation. Consequently, the M-index is an effective tool for characterizing the variations in fabric intensity among various samples or various portions of a sample.

Acknowledgements

The authors gratefully acknowledge valuable discussions with Greg Hirth and Mark Brandon, and comments on early drafts by Jeff Rahl. Comments by two anonymous reviewers helped clarify the text considerably. Brian Evans is thanked for providing the hot-pressed olivine sample. This work was supported by NSF EAR-0309448.

References

Abramson, E.H., Brown, J.M., Slutsky, L.J., Zaug, J., 1997. The elastic constants of San Carlos Olivine to 17 GPa. Journal of Geophysical Research, B, Solid Earth and Planets 102 (6), 12253–12263.

Ben Ismail, W., Mainprice, D., 1998. An olivine fabric database; an overview of upper mantle fabrics and seismic anisotropy. In: Vauchez, A., Meissner, R.O. (Eds.), Continents and Their Mantle Roots, Tectonophysics. Elsevier, Amsterdam, Netherlands, pp. 145–157.

Bunge, H., 1982. Texture Analysis in Materials Science: Mathematical Models. Butterworths, London. 593 pp.

Fliervoet, T.F., Drury, M.R., Chopra, P.N., 1999. Crystallographic preferred orientations and misorientations in some olivine rocks deformed by diffusion or dislocation creep. In: Schmid, S.M., Heilbronner, R., Stuenitz, H. (Eds.), Deformation Mechanisms in Nature and Experiment, Tectonophysics. Elsevier, Amsterdam, Netherlands, pp. 1–27.

Grimmer, H., 1979. Distribution of disorientation angles if all relative orientations of neighbouring grains are equally probable. Scripta Metallurgica 13 (2), 161–164.

Jiang, Z., Prior, D.J., Wheeler, J., 2000. Albite crystallographic preferred orientation and grain misorientation distribution in a low-grade mylonite; implications for granular flow. In: Leiss, B., Ullemeyer, K., Weber, K. (Eds.), Textures and Physical Properties of Rocks. Pergamon. Oxford International.

Jung, H., Karato, S-i., 2001. Water induced fabric transitions in olivine. Science 293, 1460–1462.

Karato, S-i., 1987. Seismic anisotropy due to lattice preferred orientation of minerals; kinematic or dynamic? In: Manghnani, M.H., Syono, Y. (Eds.), High-Pressure Research in Mineral Physics, Geophysical Monograph. American Geophysical Union, Washington, DC, United States, pp. 455–471.

Katayama, I., Jung, H., Karato, S-i., 2004. A new type of olivine fabric at modest water content and low stress. Geology 32 (12), 1045–1048.

Lapworth, T., Wheeler, J., Prior, D.J., 2002. The deformation of plagioclase investigated using electron backscatter diffraction crystallographic preferred orientation data. Journal of Structural Geology 24 (2), 387–399.

Liu, J., Chakrabarti, D.J., 1996. Grain structure and microtexture evolution during superplastic forming of a high strength Al–Zn–Mg–Cu alloy. Acta Materialia vol. 44 AD (12). Aluminum Co of America, PA, USA, pp. 4647–4661.

MacKenzie, J., Thomson, M., 1957. Some statistics associated with the random disorientation of cubes. Biometrika 44 (1/2), 205–210.

Mainprice, D., 1990. A FORTRAN program to calculate seismic anisotropy from the lattice preferred orientation of minerals. Computational Geosciences 16, 385–393.

Mainprice, D., Silver, P.G., 1993. Interpretation of SKS-waves using samples from the subcontinental lithosphere. In: Mainprice, D., Vauchez, A., Montagner, J.P. (Eds.), Dynamics of the Subcontinental Mantle; From Seismic Anisotropy to Mountain Building, Physics of the Earth and Planetary Interiors. Elsevier, Amsterdam, Netherlands, pp. 257–280.

Matthies, S., Wagner, F., 1996. On a $1/n$ law in texture related single orientation analysis. Physica Status Solidi 196.

Morawiec, A., 1995. Misorientation-angle distribution of randomly oriented symmetric objects. Journal of Applied Crystallography 28 (3), 289.

Nicolas, A., Christensen, N.I., 1987. Formation of anisotropy in upper mantle peridotites; a review. In: Fuchs, K., Froidevaux, C. (Eds.),

Composition, Structure and Dynamics of the Lithosphere–Asthenosphere System, Geodynamics Series. American Geophysical Union, Washington, DC, United States, pp. 111–123.

Prior, D.J., et al., 1999. The application of electron backscatter diffraction and orientation contrast imaging in the SEM to textural problems in rocks. American Mineralogist 84 (11–12), 1741–1759.

Samajdar, I., Doherty, R.D., 1994. Grain boundary misorientation in DC-cast aluminum alloy. Scripta Metallurgica et Materialia vol. 31 AD (5). Drexel Univ., Philadelphia, PA, USA, pp. 527–530.

Wenk, H., 1985. Preferred Orientation in Deformed Metals And Rocks: An Introduction to Modern Texture Analysis. Academic Press, Orlando. 610 pp.

Wenk, H.R., 2002. Texture and anisotropy. In: Karato, S.I., Wenk, H.R. (Eds.), Plastic Deformation of Minerals and Rocks. Mineralogical Society of America and Geochemical Society, Washington, DC, United States.

Wheeler, J., Prior, D., Jiang, Z., Spiess, R., Trimby, P., 2001. The petrological significance of misorientations between grains. Contributions to Mineralogy and Petrology 141, 109–124.